Journal of Computational Physics 405 (2020) 109111

Contents lists available at ScienceDirect

Journal of Computational Physics

www.elsevier.com/locate/jcp

Letter to the editor

Truncation errors of the D3Q19 lattice model for the lattice Boltzmann method

Martin Bauer [a,*], Goncalo Silva [b], Ulrich Rüde [a,c]

[a] Chair for System Simulation, Friedrich–Alexander–Universität Erlangen–Nürnberg, Cauerstraße 11, 91058 Erlangen, Germany
[b] LAETA, IDMEC, Mechanical Engineering Department, Instituto Superior Tecnico, University of Lisbon, P-1049001 Lisbon, Portugal
[c] CERFACS, 42 Avenue Gaspard Coriolis, 31057 Toulouse Cedex 1, France

ARTICLE INFO

Article history:
Received 24 August 2018
Received in revised form 2 October 2019
Accepted 7 November 2019
Available online 19 November 2019

ABSTRACT

We comment on the truncation error analysis and numerical artifacts of the D3Q19 lattice Boltzmann model reported in Silva et al. [3]. We present corrections for specific spatial truncation error terms in the momentum conservation equations. By introducing an improved discrete equilibrium for the D3Q19 stencil, we show that the reported spurious currents in a square channel duct flow are caused by the form of the discrete equilibrium and are not due to the structure and isotropy properties of the D3Q19 velocity set itself. Numerical experiments on a square channel and a more complex nozzle geometry confirm these results.

© 2019 Elsevier Inc. All rights reserved.

1. Truncation error analysis

We comment on the truncation error analysis and numerical artifacts of the D3Q19 lattice Boltzmann model reported in [3]. We correct the spatial truncation error terms in the momentum conservation equation (20). All following equations use the same notation as [3] with the exception of $\bar{\rho} := \rho_0$, since we reserve numeric subscripts to denote cartesian coordinates. Our result for the momentum conservation equation reads

$$\partial_i \left(\frac{p}{\bar{\rho}} \delta_{ih} + u_i u_h \right) - a_h - \frac{1}{3} c^2 \Delta t \Lambda^+ \left(\partial_i \partial_i u_h + 2 \partial_i \partial_h u_i \right) = -c^2 \Delta t^2 \left(\Lambda^{+2} - \frac{1}{12} \right) \left(\partial_i \partial_i \partial_h \left(\frac{p}{\bar{\rho}} \right) + E_h \right). \tag{1}$$

This result differs from equation (20) of the original work [3] in the form of the velocity error terms of order $c^2 \Delta t^2$, labeled E_h. We obtain

$$E_h^{\mathrm{D3Q27}} = \partial_i \partial_i \partial_j (u_h u_j) + \partial_i \partial_j \partial_h (u_i u_j) - \partial_h \partial_h \partial_h (u_h^2), \tag{2}$$

for the D3Q27 model and

$$E_h^{\mathrm{D3Q19}} = \partial_h \partial_i \partial_i (u_h^2) + 3 \partial_h \partial_h \partial_i (u_h u_i) + \delta_{ij} \partial_i \partial_i \partial_j (u_j u_h) + \delta_{ij} \partial_h \partial_i \partial_i (u_j u_j) - 5 \partial_h \partial_h \partial_h (u_h^2) - \frac{1}{2} (1 - \delta_{ij})(1 - \delta_{ih})(1 - \delta_{jh}) \partial_i \partial_i \partial_h (u_j^2), \tag{3}$$

* Corresponding author.
E-mail address: martin.bauer@fau.de (M. Bauer).

https://doi.org/10.1016/j.jcp.2019.109111
0021-9991/© 2019 Elsevier Inc. All rights reserved.

for the D3Q19 model. All equations use Einstein summation convention in the bound indices i and j. Einstein summation convention does not apply to the free index h. The speed of sound is $c_s = \sqrt{\frac{1}{3}}\mathrm{c}$. Our analysis is conducted with the open-source computer algebra system `sympy`. For reproducibility, the source code for this automated analysis is provided as additional material.

2. Improved D3Q19 equilibrium

In Silva et al. [3] the E_h terms are used to analyze the spatial truncation error of the D3Q19 and D3Q27 method. They conclude that, with the standard incompressible equilibrium [2], the observed numerical artifacts for the D3Q19 model are caused by the lack of isotropy support of the D3Q19 stencil. However, as will be detailed in a separate study, we find that the reported artifacts for the square duct experiment do not occur if the D3Q19 equilibrium is changed to

$$f_q^{(eq)} = w_q\,\rho + w_q\,\bar{\rho}\cdot\begin{cases} -u_i u_i & \mathbf{c_q} = (0,0,0) \\ 3u_i c_{qi} - 3u_i u_i + 6(u_i c_{qi})^2 & \mathbf{c_q} \in \{(\pm1,0,0),(0,\pm1,0),(0,0,\pm1)\} \\ 3u_i c_{qi} - \frac{3}{2}u_i^2 c_{qi}^2 + \frac{9}{2}(c_{qi}u_i)^2 & \text{else} \end{cases} \tag{4}$$

instead of using the standard equilibrium

$$f_q^{(eq)} = w_q\,\rho + w_q\,\bar{\rho}\cdot\begin{cases} -\frac{3}{2}u_i u_i & \mathbf{c_q} = (0,0,0) \\ 3u_i c_{qi} - \frac{3}{2}u_i u_i + \frac{5}{2}(u_i c_{qi})^2 & \mathbf{c_q} \in \{(\pm1,0,0),(0,\pm1,0),(0,0,\pm1)\} \\ 3u_i c_{qi} - \frac{3}{2}u_i u_i + \frac{9}{2}u_i u_j c_{qi} c_{qj} & \text{else} \end{cases} \tag{5}$$

The weights w_q of the improved equilibrium (4) are equal to the weights of the standard equilibrium, see (5) [1,3]. To distinguish both D3Q19 equilibria, we label the standard version D3Q19-S and our improved version D3Q19-I. The D3Q19-I model is constructed in moment space by matching discrete moments with moments of the continuous Maxwellian up to $O(u^2)$. Alternatively, this new D3Q19-I model can also be obtained by using the MRT formalism of [1] and choosing the three free parameters they introduce as $w_\epsilon = 3$, $w_{\epsilon j} = \frac{17}{2}$, and $w_{xx} = 2$. Note that the lattice structure and isotropy properties of the D3Q19 stencil remain unchanged. The error term for the D3Q19-I model reads

$$E_h^{\text{D3Q19-I}} = \partial_h\partial_i\partial_i(u_h^2) + 3\partial_h\partial_h\partial_i(u_h u_i) + \delta_{ij}\partial_i\partial_i\partial_j(u_j u_h) + \delta_{ij}\partial_h\partial_i\partial_i(u_j u_j) - 5\partial_h\partial_h\partial_h(u_h^2). \tag{6}$$

3. Numerical results

We repeat the numerical experiments for the square Poiseuille duct flow as reported in section 7.1. of [3]. As in the original work [3] we restrict ourselves to the case of a duct that is aligned with the x-axis and leave the more general case of an inclined flow to future work. As reported by [3] and confirmed here, the D3Q19-S lattice model shows spurious currents in the y-z plane. The error is measured using the maximum velocity, normal to the flow direction normalized with the maximum flow velocity: $\max(u_1)/\max(u_0)$, where the x, y and z components of the Cartesian coordinate system are labeled by the indices $(0,1,2)$. This quantity is dimensionless and therefore suited for comparing results obtained at different grid resolutions. As depicted in Fig. 1, the artifacts of the D3Q19-S model can be remedied with the improved equilibrium formulation D3Q19-I. While the D3Q19-S model has spurious currents that decrease with the resolution of the lattice, the D3Q19-I and D3Q27 models show no spurious currents up to machine precision. These results demonstrate that the artifacts can not be caused by a lack of isotropy of the D3Q19 stencil, since then the D3Q19-I model would show them as well. These numerical findings can be explained by the form of the error term E_h. Writing out the error terms without Einstein summation convention for the duct flow scenario, where the change in x direction is zero $\partial_0(\cdot) = 0$, yields

$$E^{D3Q27}\Big|_{\partial_0(\cdot)=0} = \begin{bmatrix} \partial_1\partial_1\partial_1(u_0u_1) + \partial_1\partial_2\partial_2(u_0u_1) + \partial_1\partial_1\partial_2(u_0u_2) + \partial_2\partial_2\partial_2(u_0u_2) \\ \partial_1\partial_1\partial_1(u_1^2) + \partial_1\partial_2\partial_2(u_1^2) + \partial_1\partial_2\partial_2(u_2^2) + 3\partial_1\partial_1\partial_2(u_1u_2) + \partial_2\partial_2\partial_2(u_1u_2) \\ \partial_1\partial_1\partial_2(u_1^2) + \partial_1\partial_1\partial_2(u_2^2) + \partial_2\partial_2\partial_2(u_2^2) + \partial_1\partial_1\partial_1(u_1u_2) + 3\partial_1\partial_2\partial_2(u_1u_2) \end{bmatrix} \tag{7}$$

for the D3Q27 model,

$$E^{\text{D3Q19-I}}\Big|_{\partial_0(\cdot)=0} = \begin{bmatrix} \partial_1\partial_1\partial_1(u_0u_1) + \partial_2\partial_2\partial_2(u_0u_2) \\ \partial_1\partial_1\partial_1(u_1^2) + \partial_1\partial_2\partial_2(u_1^2) + \partial_1\partial_2\partial_2(u_2^2) + 3\partial_1\partial_1\partial_2(u_1u_2) + \partial_2\partial_2\partial_2(u_1u_2) \\ \partial_1\partial_1\partial_2(u_1^2) + \partial_1\partial_1\partial_2(u_2^2) + \partial_2\partial_2\partial_2(u_2^2) + \partial_1\partial_1\partial_1(u_1u_2) + 3\partial_1\partial_2\partial_2(u_1u_2) \end{bmatrix} \tag{8}$$

for the improved D3Q19-I model, and

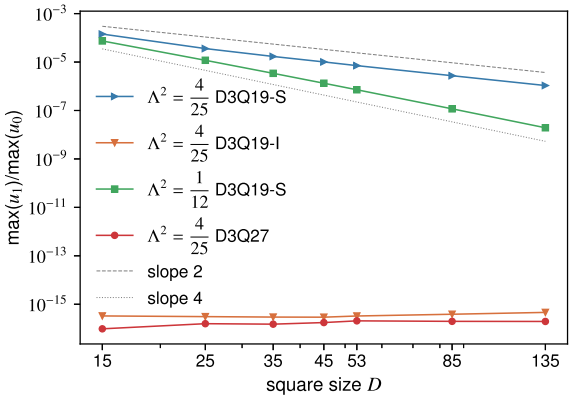

Fig. 1. Spurious currents for different lattice models in duct flow scenario - corresponds to Fig. (4a) of [3].

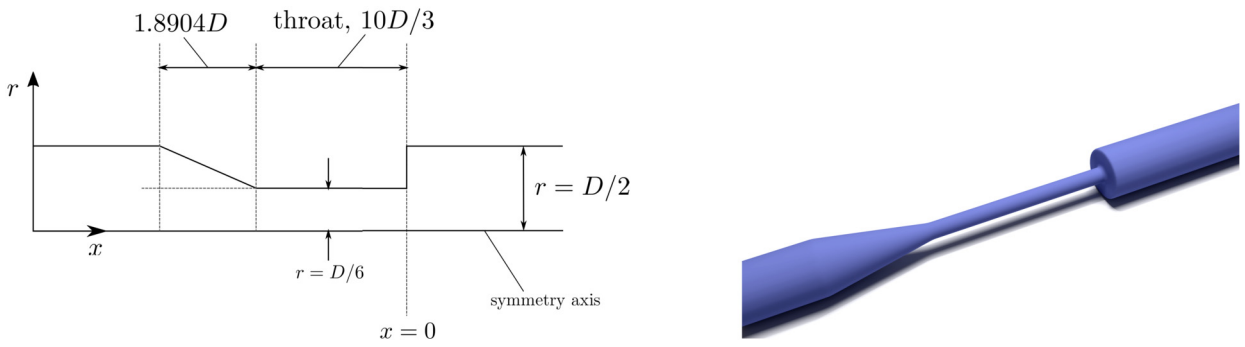

Fig. 2. Nozzle geometry for second simulation taken from [4]: specifications - not to scale (left) and rendering (right).

$$E^{\text{D3Q19-S}}\Big|_{\partial_0(\cdot)=0} = \begin{bmatrix} \partial_1\partial_1\partial_1(u_0u_1) + \partial_2\partial_2\partial_2(u_0u_2) \\ -\frac{1}{2}\partial_1\partial_2\partial_2(u_0^2) + \partial_1\partial_1\partial_1(u_1^2) + \partial_1\partial_2\partial_2(u_1^2) + \partial_1\partial_2\partial_2(u_2^2) + 3\partial_1\partial_1\partial_2(u_1u_2) + \partial_2\partial_2\partial_2(u_1u_2) \\ -\frac{1}{2}\partial_1\partial_1\partial_2(u_0^2) + \partial_1\partial_1\partial_2(u_1^2) + \partial_1\partial_1\partial_2(u_2^2) + \partial_2\partial_2\partial_2(u_2^2) + \partial_1\partial_1\partial_1(u_1u_2) + 3\partial_1\partial_2\partial_2(u_1u_2) \end{bmatrix} \tag{9}$$

for the standard D3Q19-S model. In the investigated square duct scenario, the exact solution has no transverse velocity components ($u_1 = u_2 = 0$) i.e. only u_0 is different from zero. Only in the D3Q19-S model an error term containing u_0 enters the y and z error components, whereas in the D3Q27 and the D3Q19-I model there is no influence of u_0 on the y and z errors. The highlighted terms $\partial_1\partial_2\partial_2(u_0^2)$ in (9), lead to the observed spurious currents normal to the flow direction for the standard D3Q19-S model.

The D3Q19-I equilibrium leads to more accurate results also for a practically relevant scenario of a nozzle geometry (Fig. 2) that has been employed in [4] to compare D3Q19-S and D3Q27. We use the same parametrization and evaluation parameters as in Ref. [4]. It has been shown in Ref. [4] that the D3Q19-S lattice model produces qualitatively different results than the D3Q27 model. These deficiencies were found to be independent of mesh resolution and Mach number, and thus suspected to be caused by the lack of isotropy of the D3Q19 stencil. We here reproduce and confirm the results for the standard D3Q19-S and the D3Q27 model and, additionally, conduct the simulations with the D3Q19-I lattice model. Fig. 3 shows contour plots of the velocity in flow direction u_x at a slice $x = 4D$. Due to the symmetry of the geometry we expect the laminar flow profile to be radially symmetric. While the D3Q27 solution (right) shows perfect symmetry, the standard D3Q19 lattice model yields a qualitatively different result. Despite requiring significantly less computational resources compared to the D3Q27 model, the improved D3Q19 model also correctly recovers the same radially symmetric solution.

To summarize, we have corrected the second order error terms in the momentum conservation equation from [3] and demonstrated that the observed spurious currents are not inherently caused by the structure of the D3Q19 stencil and can be remedied by a modified equilibrium.

Declaration of competing interest

The authors declare that they have no known competing financial interests or personal relationships that could have appeared to influence the work reported in this paper.

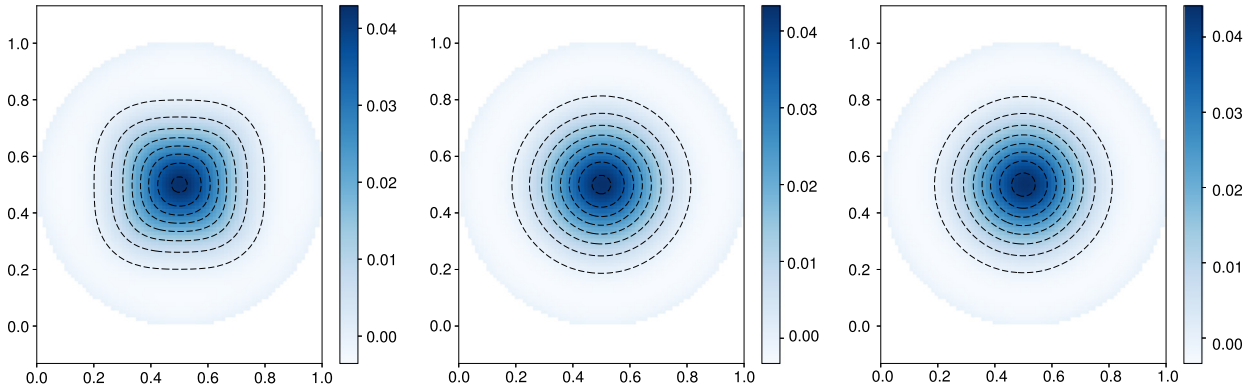

Fig. 3. Cross section at $x = 4D$ for D3Q19-S (left), D3Q19-I (middle) and D3Q27 (right) at $Re = 250$ using a pipe diameter of $D = 80$ cells.

Acknowledgements

Martin Bauer is grateful for funding received from Bundesministerium für Bildung und Forschung (BMBF) through the HPC2SE project (01ICH16003D). Goncalo Silva acknowledges Fundação para a Ciência e Tecnologia (FCT) through Grant No. SFRH/BPD/111228/2015, and FCT, through IDMEC, under LAETA, project UID/EMS/50022/2019.

Appendix A. Supplementary material

Supplementary material related to this article can be found online at https://doi.org/10.1016/j.jcp.2019.109111.

References

[1] D. D'Humières, I. Ginzburg, M. Krafczyk, P. Lallemand, L.-S. Luo, Multiple-relaxation-time lattice Boltzmann models in three dimensions, Philos. Trans. R. Soc., Math. Phys. Eng. Sci. (ISSN 1364-503X) 360 (1792) (2002) 437–451, https://doi.org/10.1098/rsta.2001.0955.

[2] X. He, L.-S. Luo, Lattice Boltzmann model for the incompressible Navier–Stokes equation, J. Stat. Phys. (ISSN 0022-4715) 88 (3/4) (1997) 927–944, https://doi.org/10.1023/B:JOSS.0000015179.12689.e4.

[3] G. Silva, V. Semiao, Truncation errors and the rotational invariance of three-dimensional lattice models in the lattice Boltzmann method, J. Comput. Phys. (ISSN 0021-9991) 269 (2014) 259–279, https://doi.org/10.1016/j.jcp.2014.03.027.

[4] A.T. White, C.K. Chong, Rotational invariance in the three-dimensional lattice Boltzmann method is dependent on the choice of lattice, J. Comput. Phys. (ISSN 0021-9991) 230 (2011) 6367–6378, https://doi.org/10.1016/j.jcp.2011.04.031.